Table 1
Comparison of DNA Yields Between Unfixed or Ethanol-Fixed Frozen Tissues and Methacarn-Fixed Wax-Embedded Tissues[a]

Tissue condition	No. of sample	DNA yield (μg/mg wet tissue)
Unfixed frozen	5	1.05 ± 0.10
Ethanol-fixed frozen	5	1.15 ± 0.11
Methacarn-fixed wax-embedded	4	0.76 ± 0.06[b]

[a]Rat liver tissue was used as described previously in **ref. *15***. After dewaxing, extraction of DNA from methacarn-fixed wax-embedded small liver tissue blocks was performed by digestion with 500 μL of 10 m*M* Tris-HCl (pH 8.0), 150 m*M* NaCl, 10 m*M* ethylenediaminetetraacetic acid, 0.1% sodium dodecyl sulfate, and 1 U of proteinase K at 55°C for 2 h. The film was removed from the tube at this time point. Then 500 μL of Tris buffer-saturated phenol was added, mixed well, and centrifuged at 10,000*g* for 15 min. The supernatant was further extracted again with 500 μL of Tris-phenol/chloroform (1:1), and the separated aqueous portion after centrifugation was transferred to a new tube and treated with 0.5 U of RNase A at 37°C for 1 h. The solution was extracted with 500 μL of phenol/chloroform (1:1) and then treated with ether. Extracted DNA was precipitated by adding 1 μL of cold 99.5% ethanol, and after storing at –20°C overnight, centrifuged at 5000*g* for 5 min. The pellet was washed twice with 75% ethanol, dried, and resuspended in 10 μL of water. One milliliter of sample was used to measure DNA concentration by Hoechst 33258 and a fluorescence spectrophotometer. Extraction of DNA from methacarn-fixed wax-embedded small liver tissue blocks was performed after dewaxing. Frozen tissue blocks of unfixed or ethanol-fixed liver were directly subjected to DNA extraction, and dewaxed blocks of methacarn-fixed wax-embedded liver tissue were air-dried before extraction.

[b]Significantly different from unfixed frozen sample ($p < 0.01$ by ANOVA).

(Reproduced with permission from **ref. *15***.)

The yield and quality of extracted DNA are critical for the subsequent analysis of microdissected cells. DNA yield from ethanol-fixed frozen tissues is similar to that from unfixed frozen tissues (*see* **Table 1**) ***(15)***. On the other hand, DNA yield from methacarn-fixed wax-embedded tissue is slightly reduced, the mean value being about 70% of that from unfixed frozen tissues (**Table 1**). The integrity of extracted DNA from methacarn-fixed wax-embedded tissue is assessed by electrophoresis on 1.5% agarose gel (*see* **Fig. 1**). Although a slightly greater intensity at the top of the DNA smear is observed in unfixed or ethanol-fixed frozen samples, DNA in every case distributes within the high molecular weight range, suggesting good preservation of extracted DNA.

3.1.2. Preparation of Methacarn-Fixed Wax-Embedded Tissue Sections

1. Section at 5–10 μm in thickness using a microtome.
2. Stretch sections with slide warmer (Sakura Finetek Japan).
3. Mount stretched section onto a 1.35-μm thin polyethylene film (PALM GmbH) overlaid on a glass slide.

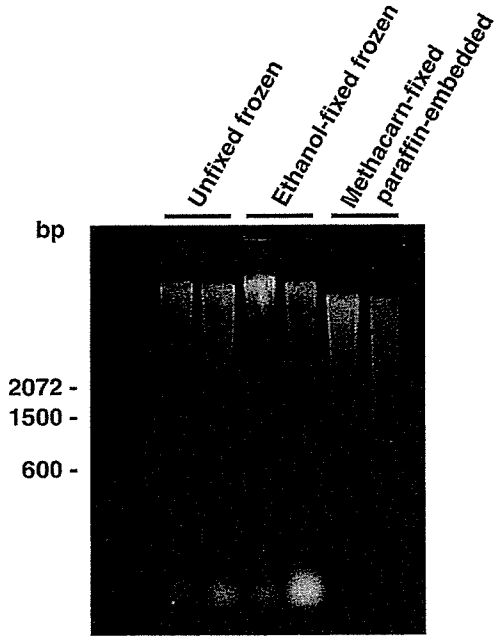

Fig. 1. Comparison of the integrity of DNA extracted from rat liver of unfixed or ethanol-fixed frozen tissue blocks and dewaxed methacarn-fixed tissue blocks. Tissue blocks were directly subjected to DNA extraction as described in the footnote of **Table 1**, and 2.0 μg of extracted DNA was subjected to electrophoresis in 1.5% agarose gel and stained with ethidium bromide as previously described *(15)*. (Reproduced with permission from **ref. 15**.)

4. Dry sections overnight at 37°C in an incubator.
5. Store sections at 4°C until use.

3.2. Tissue Staining

Dewax sections by immersing in xylene for 3 × 2 min followed by 99.5% ethanol for 2 × 2 min. Tissue sections can be stained with cresyl violet or H&E, or immunostained (*see* **Note 2**).

3.2.1. Cresyl Violet Staining

1. Dissolve 0.5 g cresyl violet in 500 mL water.
2. Add 8 drops of acetic acid.
3. If necessary, boil the solution until completely dissolved.
4. Filter the solution before using.
5. Immerse dewaxed sections briefly in water.

6. Incubate sections in cresyl violet solution for 20 min.
7. Wash sections once with 95% ethanol that contains 0.5% acetic acid, and then with 99.5% ethanol twice.
8. Air-dry.

3.2.2. Hematoxylin and Eosin Staining

1. Immerse dewaxed sections briefly in water.
2. Immerse sections in hematoxylin solution (Tissue-Tek® Hematoxylin 3G) for 10 s.
3. Wash sections briefly with water.
4. Immerse sections with eosin solution (Tissue-Tek® Eosin) for 10 s.
5. Wash sections briefly with 99.5% ethanol.
6. Air-dry.

3.2.3. Immunostaining

1. Treat dewaxed sections with 1% periodic acid solution for 10 min.
2. Wash sections briefly with water and 1X phosphate-buffered saline (PBS; pH 7.4).
3. Block nonspecific binding sites with 0.5% casein in PBS for 30 min.
4. Incubate with primary antibody of appropriate dilution for 2 h.
5. Wash sections with PBS for 5 min × 3.
6. Incubate sections with biotin-labeled secondary antibody.
7. Repeat **step 5**.
8. Incubate sections with avidin-biotin complex utilizing Vectastain Elite kit (Vector Laboratories).
9. Repeat **step 5**.
10. Visualize immunoreaction using the avidin/biotin system with 0.004% hydrogen peroxide as substrate and DAB as chromogen.
11. Rinse sections with water.
12. Perform nuclear staining with hematoxylin if desired (*see* **Subheading 3.2.2.**).
13. Air-dry.

Tissue staining can affect the yield and quality of extracted DNA with methacarn-fixed wax-embedded tissue sections (*see* **Table 2** and **Fig. 2**) ***(15)***. **Table 2** shows the DNA yield from methacarn-fixed wax-embedded tissue sec-

Fig. 2. (*opposite page*) Integrity of DNA extracted from stained sections of methacarn-fixed wax-embedded tissue. Liver of a rat treated with thioacetamide at the promotion stage in the two-stage hepatocarcinogenesis model ***(23,24)*** was used. Tissue blocks were trimmed to obtain sections of 100 mm^2 in area before sectioning, and sectioned at 10 μm in thickness. Serial sections were randomized and mounted onto polyethylene film overlaid on a glass slide. Dewaxed sections were either unstained, stained with H&E, or immunostained with glutathione-*S*-transferase placental form

Table 2
Effect of Staining on Yield of Extracted DNA From Methacarn-Fixed Rat Liver Wax-Embedded Tissue Sections[a]

Tissue condition	No. of samples	Yield of DNA (ng/100 mm^2 area)[b]	Ratio of unstained section (%)
Unstained	10	2705.1 ± 853.4	100
H&E-stained	5	2687.4 ± 632.4	99.3
Immunostained[c]	13	314.5 ±85.2[d]	11.6

[a]Liver of a rat treated with thioacetamide at the promotion stage in the two-stage hepatocarcinogenesis model *(23,24)* was used as described previously in **ref. *15***.

[b]Tissue blocks were trimmed to 100 mm^2 before sectioning, and sectioned at 10 μm. DNA extraction and estimation of its concentration were performed according to the methods described in **Table 1**.

[c]Sections were immunostained with GST-P.

[d]Significantly different from the unstained and H&E-stained samples ($p < 0.0001$ by ANOVA).

(Reproduced with permission from **ref. *15***.)

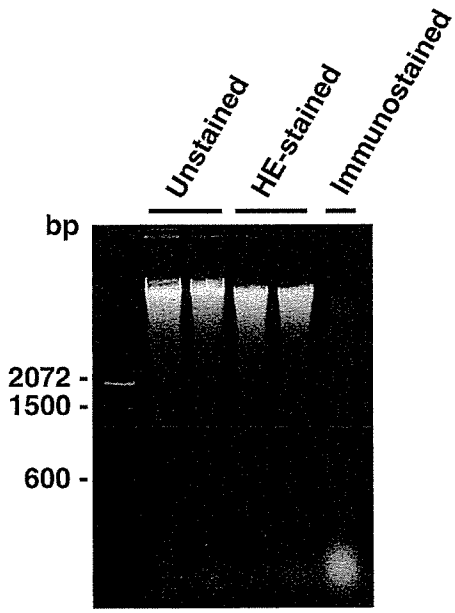

Fig. 2. (*continued*) (GST-P) (*see* **Subheadings 3.2.2.** and **3.2.3.**). One μg of extracted DNA from whole tissue section was subjected to electrophoresis in 1.5% agarose gel and stained with ethidium bromide as described previously ***(15)***. (Reproduced with permission from **ref. *15***.)

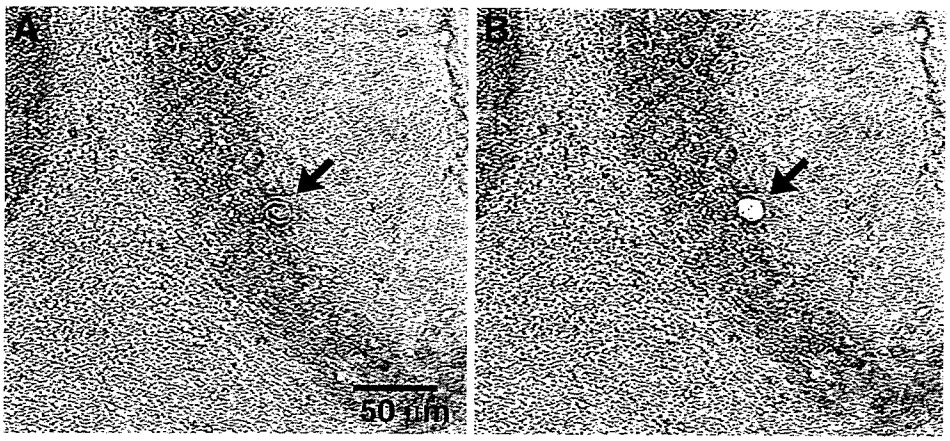

Fig. 3. Microdissection of single Purkinje cells from cresyl violet-stained rat cerebellum section as described previously in **ref. *15***. (**A**) Wax-embedded rat cerebellum sectioned at 10 µm in thickness was mounted on a film, dewaxed, and stained with cresyl violet (*see* **Subheading 3.2.1.**). A single Purkinje cell was selected and microdissected from the surrounding tissue with a laser beam (arrow). (**B**) The Purkinje cell has been cut out and catapulted by laser pressure (arrow). (Reproduced with permission from **ref. *15***.)

tions after tissue staining. The yield recovered from H&E-stained sections is similar to that from unstained sections. Immunostained tissue sections, on the other hand, result in very low DNA yield, values being 12% those of unstained sections. **Fig. 2** shows the integrity of DNA extracted from stained sections as visualized by electrophoresis on 1.5% agarose gel. DNA from unstained sections distributes mainly within the high molecular weight range. Similar to the unstained tissue section, H&E-stained sections show good preservation of the extracted DNA. As compared to unstained and H&E-stained cases, DNA extracted after immunostaining shows significant degradation of the DNA with small DNA fragments of approx 100 bp size (*see* **Note 3**).

3.3. Microdissection

Microdissection is performed with PALM Robot-MicroBeam equipment (Carl Zeiss Co., Ltd.) as described previously (*see* **Note 4**) ***(25)***. Briefly, the film with the attached specimen is mounted in reverse (film side up) onto a new cover slip (26 × 76 mm) by adhering the film to the cover slip with nail polish. The specimens are then subjected to Robot-MicroBeam dissection by laser beam and the selected cells are catapulted by laser pressure into mineral oil-coated PCR tube caps (**Fig. 3**) ***(15)***. In case of large specimens (circle areas of 150–200 µm in radius or square areas larger than 60 × 60 µm), the excised

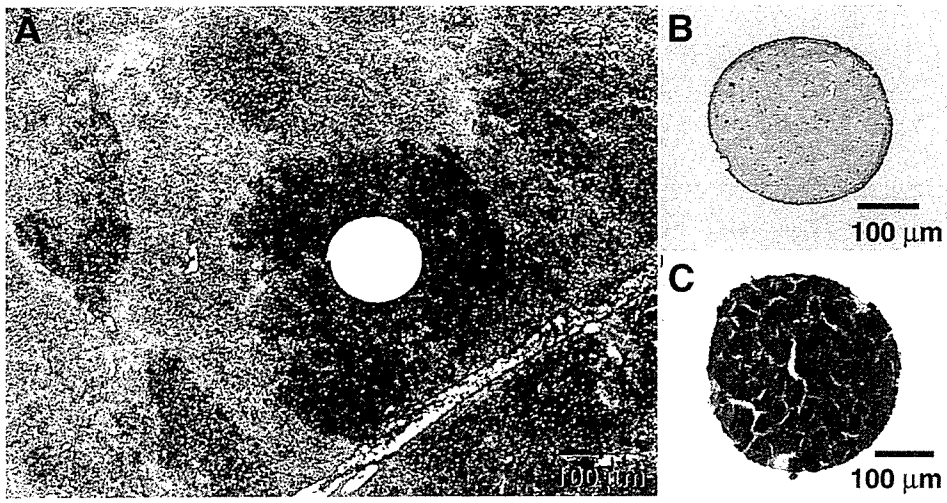

Fig. 4. Microdissection using a liver section immunostained with GST-P from a thioacetamide-treated rat in the two-stage hepatocarcinogenesis model as described previously in **ref. *15***. (**A**) A liver section (10-μm thick) mounted on polyethylene film was immunostained with GST-P (*see* **Subheading 3.2.3.**) and a circle area of 150 μm radius within a GST-P-positive focus was microdissected. (**B**) Removed GST-P-positive cellular area from the section shown in **Fig. 4A**. (**C**) Identical portions of circle area in GST-P-positive foci were microdissected from H&E-stained adjacent section. A mean of 150 cells were contained in the circle area ($n = 5$). (Reproduced with permission from **ref. *15***.)

cells can be picked up with a thin needle tip (**Fig. 4**) *(15)*. Transfer of microdissected specimen on the cap of a PCR tube should be verified under a microscope.

3.4. DNA Extraction From Microdissected Cells

Microdissected cells or tissue areas on PCR tube caps are subjected to extraction with 4 μL of TaKaRa DEXPAT™ (*see* **Note 5**) at 95°C for 10 min, and the entire extracts are used as a template for PCR by adding to the master mix of total 50 μL directly as described in **Subheadings 3.5.1.** and **3.5.2.** *(15)*. In the case of a large cellular area such as 1 × 1 mm area, tissue specimens are extracted with 40 μL of DEXPAT.

3.5. PCR

PCR is the major tool for analysis of genomic DNA; cycle numbers should be minimized to avoid amplification-derived DNA-polymerization errors. Hot-start PCR of the genomic sequence of the gene of interest is performed with

PLATINUM *Taq* DNA polymerase in a 50-μL total reaction volume *(15)*. If nested PCR is intended, 1 μL of the first PCR product is used as a template in a 20-μL total volume (*see* **Note 6**).

3.5.1. Amplification by Nested PCR

1. Aliquot 4 μL of extracted DNA and mix with PCR reaction mixture contained 20 m*M* Tris-HCl (pH 8.4), 50 m*M* KCl, 0.2 m*M* dNTP, 1.5 m*M* $MgCl_2$, 0.2 μ*M* each primer, and 2.5 U of *Taq* DNA polymerase in a 50-μL total volume.
2. Perform first-step PCR of 20–35 cycles.
3. Aliquot 1 μL of the first PCR product and mix with PCR reaction mixture with 1 U of PLATINUM *Taq* DNA polymerase in a 20-μL total volume.
4. Perform second-step PCR of 20–35 cycles.
5. Aliquot 8 μL of the PCR product and run agarose gel electrophoresis to identify the amplified target fragment (*see* **Fig. 5**).
6. Aliquot 10 μL of the PCR product for direct sequencing.

By nested PCR, the 522-bp DNA fragment of the α_{2u}-globulin gene is successfully amplified in 20% of the PCR attempts of single Purkinje cells with a total of 70 PCR cycles from cresyl violet-stained rat cerebellum sections (*see* **Table 3**) *(15)*. Similar, but less effective, amplification can be obtained with microdissected areas of hippocampal CA1 region, in which a successful detection is obtained in 15% of 20 × 20 μm samples (corresponding to 2.4 cells). The frequency of PCR detection increases with the area microdissected, but does not reach 100% even in a 60 × 60 μm area.

3.5.2. Amplification by Single-Step PCR

1. Aliquot 4 μL of extracted DNA and mix with PCR reaction mixture as described in **Subheading 3.5.1.** and 2.5 U of *Taq* DNA polymerase in a 50-μL total volume.
2. Perform PCR of 35 cycles.
3. Aliquot 8 μL of the PCR product and run agarose gel electrophoresis to identify the amplified target fragment.
4. Aliquot 10 μL of the PCR product for direct sequencing.

In the PALM system, either a rectangle or a circle of any size can be microdissected in automated mode. In H&E-stained rat liver sections as described in **Fig. 4**, a 522-bp fragment can be amplified by single-step PCR of 35 cycles with both 150- and 200-μm-radius samples after DEXPAT extraction, although the amplification of 969-bp fragments is unsuccessful even with 200-μm-radius samples (*see* **Table 4**) *(15)*. Liver samples of 150- and 200-μm-radius areas in this case contain 150 and 270 cells, respectively. In immunostained tissue, a weak 522-bp band can be amplified only with 200-μm-radius samples. In the case of 150-μm-radius samples, only a 184-bp fragment can be amplified.

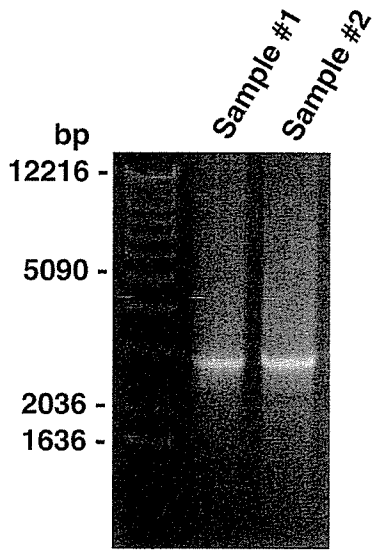

Fig. 5. Nested PCR results for the α_{2u}-globulin genomic sequence (Accession no. M24108 in GenBank/EMBL Data Bank), sized 2.8 kb, with DNA extracted from methacarn-fixed wax-embedded rat cerebral cortex as described previously *(15)*. From 10-μm thick, cresyl violet-stained brain sections, 1 × 1 mm areas of cerebral cortex were microdissected and extracted with 40 μL of DEXPAT to extract DNA. Four-μL aliquots of cell extracts were directly applied for the first PCR reaction with upstream-outside primer, 5'-ACGGATCCAG GCTTCAAGTT CCGTATTA-3' and downstream primer for the 2954-bp fragment, 5'-TGAAATCCTG AGACTAAGCT-3'. With 1 μL of the first PCR product, second-step PCR was performed to amplify a 2.8-kb fraction with a combination of upstream-inside primer, 5'-AAAGTTAAAT GGAATCAGAA-3', and the downstream primer used for the 2954-bp fragment in the first PCR. Nested PCR in a 20-μL total volume was performed using 1 μL of the first PCR product as a template. This figure shows results of two different samples. (Reproduced with permission from **ref. *15***.)

4. Notes

1. Exposure of tissues to saline prior to fixation may cause a severe tissue shrinkage artifact *(10)*. Glassware for the preparation of methacarn should be autoclaved before use. Do not use disposable plasticware that can be damaged by chloroform for the preparation and/or storage of methacarn solution. For fixation, the ratio of the fixative volume to tissue volume should be 20:1–30:1. If necessary, tissue processing can be stopped at the step of ethanol dehydration, and tissue blocks can be kept in ethanol at 4°C for several days after fixation.
2. Immersion of the tissue section in aqueous solution for a long time may increase the risk of degradation of DNA *(15)*. If nuclear staining is intended, the staining

Table 3
Detection of 522-bp DNA Fragment From Microdissected Single Cells or Cellular Areas by Nested PCR[a]

Cell or cellular area	Microdissected	No. of samples	PCR-detection (%)
Purkinje cell	single cell	15	20
Hippocampus,	20 × 20 μm (2.4 cells)[b]	26	15
CA1 region	40 × 40 μm (9.5 cells)[b]	15	67
	60 × 60 μm (21.3 cells)[b]	15	87
Cerebral cortex[c]	1 × 1 mm	24	100

[a]Rat α_{2u}-globulin gene was used for PCR as described previously in **ref. *15***. First-step PCR was performed to amplify a 969-bp fragment with an upstream-outside primer, 5'-ACGGATCCAG GCTTCAAGTT CCGTATTA-3', and a downstream primer, 5'-CGTCATCTGT GGAGGAAATT-3'. With 1 μL of the first PCR product, second-step was performed to amplify a 522-bp fragment with an upstream-inside primer, 5'-AAAGTTAAAT GGAATCAGAA-3', and a downstream-inside primer, 5'-TAAGTCCGTC TCACATGGCT-3'.

[b]Mean cell number in a 60 × 60 μm area (n = 18) was estimated with the aid of an objective micrometer, and the mean cell number in each square area was calculated.

[c]Extract from 1 × 1 mm area of cerebral cortex was further diluted with DEXPAT to adjust the concentration of template to correspond to a 60 × 60 μm area for first-step PCR.

(Reproduced with permission from **ref. *15***.)

solution should be autoclaved or filtrated if possible. Methacarn-fixed tissue sections can be stained more quickly than formalin-fixed tissue sections, and therefore the time of the histological staining procedure can be reduced.

3. Immunostaining of methacarn-fixed wax-embedded tissue results in a substantial decrease in DNA yield, in particular the loss of high molecular weight DNA. There is progressive decrease in DNA yield in proportion to the length of the immunostaining process ***(15)***.
4. There are two major techniques for microdissection utilizing the precision of lasers. One technique is laser microbeam microdissection as employed in our laboratory; this system is based on a pulsed UV laser with a small beam focus to cut out areas or cells of interest by photoablation of adjacent tissue. Another technique is laser capture microdissection, which uses a low-energy infrared laser pulse to capture the targeted cells by focal melting of the thermoplastic membrane through laser activation. Advantages and disadvantages of these systems are described elsewhere ***(26)***.
5. TaKaRa DEXPAT is a reagent originally designed for one-step extraction of DNA from wax-embedded tissue fixed with 10% formalin. DEXPAT is designed to optimize DNA extraction from wax embedded tissue; it utilizes ion exchange resin and detergents, and DNA is extracted in the supernatant. We use only the detergent component.With methacarn-fixed wax-embedded tissues, the time for the preparation of PCR-ready DNA from wax-embedded tissue is dramatically reduced from 2 to 3 d required for a conventional method for formalin-fixed tissues to 25 min.

Table 4
Detection of Genomic DNA Fragment by Single-Step PCR in H&E-Stained or Immunostained Tissue Areas From Methacarn-Fixed Rat Liver Wax-Embedded Tissue Sections[a]

Stain	Tissue area (μm in radius)	Fragment size (bp)	Positive detection
H&E-stained	200	184[b]	8/8 (100%)
	200	522[c]	9/9 (100%)
	200	969[c]	0/8 (0%)
	150	184	5/5 (100%)
	150	522	5/5 (100%)
Immunostained[d]	200	184	5/5 (100%)
	200	522	5/5 (100%)
	150	184	10/10 (100%)
	150	522	0/5 (0%)

[a]Liver of a rat treated with thioacetamide at the promotion stage in the two-stage hepatocarcinogenesis model was used as described previously in **ref. *15***. Circle areas of 150 or 200 μm in radius were microdissected and solubilized with 4 μL of DEXPAT solution in PCR tubes at 95°C for 10 min and whole extracts were subjected to PCR directly. PCR with 50 μL reaction volume was performed to amplify 184-, 522-, and 969-bp fragments with the same cycle parameters of 95°C for 2 min, 35 cycles of 95°C for 1 min, 55°C for 1 min, and 72°C for 30 s, and final extension at 72°C for 7 min. Eight microliters of PCR product was applied to 2.0% agarose gel electrophoresis.

[b]Rat GST-P gene (Accession no. L29427 in GenBank/EMBL Data Bank) was amplified using upstream primer, 5'-GGAGCAGGAC CCAAAAATGA-3', and downstream primer, 5'-GCA GACGAAT AAAGGCCCCA-3'.

[c]Rat α_{2u}-globulin gene was used for amplification. Primer pairs for each DNA fragment were similar to those described in the footnote of **Table 3**.

[d]Sections were immunostained with GST-P.

(Reproduced with permission from **ref. *15***.)

6. To amplify target fragment sizes smaller than 1 kb, PCR was performed with cycle parameters of 95°C for 5 min, 35 cycles of 95°C for 1 min, 55°C for 1 min, 72°C for 30 s. The extension time for 2, 3, and 4 kb is 1.5, 2.5, and 3.5 min respectively. Although the source of cells and the detection system are different from those in the present study, similar performance was obtained when DNA from 25 cells of alcohol-fixed cytology specimens was used in the multiplex PCR *(27)*.

Acknowledgments

This work was supported in part by Health and Labour Sciences Research Grants (Risk Analysis Research on Food and Pharmaceuticals) from the Ministry of Health, Labour, and Welfare of Japan.

References

1. Rupp, G. M. and Locker, J. (1988) Purification and analysis of RNA from paraffin-embedded tissues. *Biotechniques* **6,** 56–60.
2. Stanta, G. and Schneider, C. (1991) RNA extracted from paraffin-embedded human tissues is amenable to analysis by PCR amplification. *Biotechniques* **11,** 304–308.
3. Finke, J., Fritzen, R., Ternes, P., Lange, W., and Dolken, G. (1993) An improved strategy and a useful housekeeping gene for RNA analysis from formalin-fixed, paraffin-embedded tissues by PCR. *Biotechniques* **14,** 448–453.
4. Ikeda, K., Monden, T., Kanoh, T., et al. (1998) Extraction and analysis of diagnostically useful proteins from formalin-fixed, paraffin-embedded tissue sections. *J. Histochem. Cytochem.* **46,** 397–403.
5. Shibutani, M., Uneyama, C., Miyazaki, K., Toyoda, K., and Hirose, M. (2000) Methacarn fixation: a novel tool for analysis of gene expressions in paraffin-embedded tissue specimens. *Lab. Invest.* **80,** 199–208.
6. Shibata, D. (1994) Extraction of DNA from paraffin-embedded tissue for analysis by polymerase chain reaction: new tricks from an old friend. *Hum. Pathol.* **25,** 561–563.
7. Frank, T. S., Svoboda-Newman, S. M., and Hsi, E. D. (1996) Comparison of methods for extracting DNA from formalin-fixed paraffin sections for nonisotopic PCR. *Diagn. Mol. Pathol.* **5,** 220–224.
8. Poncin, J., Mulkens, J., Arends, J. W., and de Goeij, A. (1999) Optimizing the APC gene mutation analysis in archival colorectal tumor tissue. *Diagn. Mol. Pathol.* **8,** 11–19.
9. Uneyama, C., Shibutani, M., Nakagawa, K., Masutomi, N., and Hirose, M. (2000) Methacarn, a fixation tool for multipurpose gene expression analysis from paraffin-embedded tissue materials. *Current Topics in Biochem. Res.* **3,** 237–242.
10. Puchtler, H., Waldrop, F. S., Meloan, S. N., Terry, M. S., and Conner, H. M. (1970) Methacarn (Methanol-Carnoy) fixation. Practical and theoretical considerations. *Histochemie* **21,** 97–116.
11. Mitchell, D., Ibrahim, S., and Gusterson, B. A. (1985) Improved immunohistochemical localization of tissue antigens using modified methacarn fixation. *J. Histochem. Cytochem.* **33,** 491–495.
12. Dietmaier, W., Hartmann, A., Wallinger, S., et al. (1999) Multiple mutation analyses in single tumor cells with improved whole genome amplification. *Am. J. Pathol.* **154,** 83–95.
13. Murase, T., Inagaki, H., and Eimoto, T. (2000) Influence of histochemical and immunohistochemical stains on polymerase chain reaction. *Mod. Pathol.* **13,** 147–151.
14. Hirose, Y., Aldape, K., Takahashi, M., Berger, M. S., and Feuerstein, B. G. (2001) Tissue microdissection and degenerate oligonucleotide primed-polymerase chain reaction (DOP-PCR) is an effective method to analyze genetic aberrations in invasive tumors. *J. Mol. Diagn.* **3,** 62–67.

15. Uneyama, C., Shibutani, M., Masutomi, N., Takagi, H., and Hirose, M. (2002) Methacarn fixation for genomic DNA analysis in microdissected paraffin-embedded tissue specimens. *J. Histochem. Cytochem.* **50,** 1237–1245.
16. Pontén, F., Williams, C., Ling, G., et al. (1997) Genomic analysis of single cells from human basal cell cancer using laser-assisted capture microscopy. *Mutat. Res.* **382,** 45–55.
17. Burton, M. P., Schneider, B. G., Brown, R., Escamilla-Ponce, N., and Gulley, M. L. (1998) Comparison of histologic stains for use in PCR analysis of microdissected, paraffin-embedded tissues. *Biotechniques* **24,** 86–92.
18. Alcock, H. E., Stephenson, T. J., Royds, J. A., and Hammond, D. W. (1999) A simple method for PCR based analyses of immunohistochemically stained, microdissected, formalin fixed, paraffin wax embedded material. *Mol. Pathol.* **52,** 160–163.
19. Fend, F., Emmert-Buck, M. R., Chuaqui, R., et al. (1999) Immuno-LCM: laser capture microdissection of immunostained frozen sections for mRNA analysis. *Am. J. Pathol.* **154,** 61–66.
20. Serth, J., Kuczyk, M. A., Paeslack, U., Lichtinghagen, R., and Jonas, U. (2000) Quantitation of DNA extracted after micropreparation of cells from frozen and formalin-fixed tissue sections. *Am. J. Pathol.* **156,** 1189–1196.
21. Gjerdrum, L. M., Lielpetere, I., Rasmussen, L. M., Bendix, K., and Hamilton-Dutoit, S. (2001) Laser-assisted microdissection of membrane-mounted paraffin sections for polymerase chain reaction analysis: identification of cell populations using immunohistochemistry and *in situ* hybridization. *J. Mol. Diagn.* **3,** 105–110.
22. Shibutani, M. and Uneyama, C. (2002) Methacarn, a fixation tool for multipurpose genetic analysis from paraffin-embedded tissues, in *Methods in Enzymology* (Conn, M., ed.), Academic Press, New York, vol. 356, pp. 114–125.
23. Shirai, T. (1997) A medium-term rat liver bioassay as a rapid in vivo test for carcinogenic potential: a historical review of model development and summary of results from 291 tests. *Toxicol. Pathol.* **25,** 453–460.
24. Ito, N., Imaida, K., Asamoto, M., and Shirai, T. (2000) Early detection of carcinogenic substances and modifiers in rats. *Mutat. Res.* **462,** 209–217.
25. Schütze, K. and Lahr, G. (1998) Identification of expressed genes by laser-mediated manipulation of single cells. *Nature Biotechnol.* **16,** 737–742.
26. Fend, F. and Raffeld, M. (2000) Laser capture microdissection in pathology. *J. Clin. Pathol.* **53,** 666–672.
27. Euhus, D. M., Maitra, A., Wistuba, I. I., et al. (1999) Use of archival fine-needle aspirates for the allelotyping of tumors. *Cancer* **87,** 372–379.

Available online at www.sciencedirect.com
SCIENCE DIRECT®
Toxicology 207 (2005) 419–436
TOXICOLOGY
www.elsevier.com/locate/toxicol

Molecular pathological analysis on the mechanism of liver carcinogenesis in dicyclanil-treated mice

Mitsuyoshi Moto[a,b,*], Miwa Okamura[a,b], Tomoko Muto[c], Yoko Kashida[a], Noboru Machida[a], Kunitoshi Mistumori[a]

[a] *Laboratory of Veterinary Pathology, Tokyo University of Agriculture and Technology, 3-5-8 Saiwai-cho, Fuchu-shi, Tokyo 183-8509, Japan*
[b] *Pathogenetic Veterinary Science, United Graduate School of Veterinary Sciences, Gifu University, 1-1 Yanagido, Gifu-shi, Gifu 501-1193, Japan*
[c] *Department of Pharmacology and Toxicology, Kyorin University School of Medicine, 6-20-2 Shinkawa-cho, Mitaka-shi, Tokyo 181-8611, Japan*

Received 7 September 2004; received in revised form 26 October 2004; accepted 27 October 2004
Available online 8 December 2004

Abstract

To investigate the mechanism of hepatocarcinogenesis due to dicyclanil (DC), an insect growth regulator for sheep, histopathological and molecular biological analyses were performed in the liver of male ICR mice fed on a diet containing 1500 ppm of DC for 2 weeks (Experiment I; Exp. I). In gene expression analyses using a large-scale cDNA microarray and RT-PCR, fluctuations of expressions of metabolism-/oxidation-/reduction-related genes, such as *CYP1A*, aldehyde dehydrogenase family 1 subfamily A1 (*Aldh1a1*), and thioredoxin reductase 1 (*Txnrd1*), were predominantly observed in the liver of the DC-treated group. In Experiment II (Exp. II), small-scale and metabolism/oxidative stress-specific cDNA microarray, real-time RT-PCR, and measurement of NF-κB protein were performed in the mice liver using a two-stage hepatocarcinogenesis model, in which the male ICR mice were fed on a diet containing 1500 ppm of DC for 7 weeks after a single injection of dimethylnitrosamine (DMN). These mice were subjected to two-thirds partial hepatectomy (PH) at week 3. During histopathological examinations, a remarkable increase in γ-glutamyltransferase-positive cells was observed in the DMN + DC + PH group. During the microarray and PCR analyses, the metabolism and oxidative stress-related genes, such as *Cyp1a*, P450 oxidoreductase (*Por*), and thioredoxin reductase 1 (*Txnrd1*); a few DNA damage/repair genes, such as 8-oxoguanine DNA-glycosylase 1 (*Ogg1*); and growth arrest and DNA-damage-inducible 45 alpha (*Gadd45a*), were fluctuated in this group, together with a slight increase in the concentration of activated NF-κB. These results suggest that DNA damages due to oxidative stress may be involved in the mechanism of DC-induced hepatocarcinogenesis in mice.

Keywords: Dicyclanil; Microarray; Liver carcinogenesis; Oxidative stress; Mouse

* Corresponding author. Tel.: +81 42 367 5771; fax: +81 42 367 5771.
E-mail address: m-moto@cc.tuat.ac.jp (M. Moto).

0300-483X/$ – see front matter © 2004 Elsevier Ireland Ltd. All rights reserved.
doi:10.1016/j.tox.2004.10.011

1. Introduction

Dicyclanil (DC), 4,6-diamino-2-cyclopropylamino-pyrimidine-5-carbonitrile, is a pyrimidine-derived insect growth regulator inhibiting the molting and development of insecticides, and is used in a veterinary field for the prevention of myiasis (fly-strike) in sheep. As a result, small amounts of the parent drug and its metabolites are sometimes detected as residues in the edible tissues of these sheep (WHO, 2000). In an 18-month study conducted on the carcinogenicity of DC, it was observed that the incidence of hepatocellular carcinomas was increased in mice fed on a diet containing 1500 ppm of DC; hepatocellular necrosis was also observed in the groups fed with 100 ppm or more of DC (WHO, 2000). On the other hand, in studies conducted on the genotoxicity of DC, negative results were obtained from the in vivo and in vitro tests, and it was evaluated by the 54th meeting of the Joint FAO/WHO Expert Committee on Food Additives (JECFA) that DC is a non-genotoxic carcinogen (WHO, 2000). Additionally, our recent study indicated that negative results were obtained when a single oral administration of DC was performed in the in vivo comet assay using mice and in vivo liver initiation assay using rats, and these results support the evaluation of the JECFA (Moto et al., 2003). Therefore, it was postulated that the DC treatment-induced enhancement of hepatocarcinogenesis resulted from non-genotoxic mechanisms or tumor-promoting actions such as the enhancement of cell proliferation, inhibition of apoptosis, disorder of the cell cycle regulation, secondary genotoxicity, and so on. However, detailed investigations of molecular events in the DC-induced mice liver have not yet been performed.

In the studies conducted to evaluate the mechanism of chemical carcinogenesis, it is extremely important to understand the molecular events during the chemical-induced initiation and promotion phases in the target organs, because gene alterations may vary with the presence or absence of mutated cells and/or preneoplastic foci. Recently, large-scale gene expression analyses by the cDNA microarray have been applied in the fields of toxicology and carcinogenicity (Afshari et al., 1999; Irwin et al., 2004). Microarray analyses have been used to investigate the molecular events in the non-genotoxic carcinogens during the various stages of carcinogenesis, and the molecular events on tumor promoting mechanisms have also been reported (Chen et al., 2001; Iida et al., 2003; Kinoshita et al., 2003; Kato et al., 2004). Several non-genotoxic carcinogens are known to show tumor-promoting activities in the two-stage (initiation-promotion) carcinogenesis models (Shirai, 1997; Shibutani et al., 2002). Therefore, the presently discussed carcinogenesis model is believed to be useful in the detection of molecular profiles during the tumor promotion stage.

In the present study, to clarify the enhancement mechanism of hepatocarcinogenesis in DC-induced mice, a large-scale cDNA microarray (3800 genes) was performed to obtain primary information on molecules and/or molecular events associated with the enhancement of hepatocarcinogenesis in mice liver at the early stage of the toxicity and carcinogenicity of DC. Based on the results obtained from this microarray, a low-density and pathway-specific microarray (112 genes) were performed to investigate the details of the molecular events during the tumor promotion phase of DC using the two-stage hepatocarcinogenesis model in mice with partial hepatectomy. In addition, to clarify the mechanism of the tumor promoting effect of DC, further analyses comprising RT-PCR or real-time RT-PCR, histological examinations, and measurements of proteins associated with the pathway were carried out by taking into account the results obtained from the microarray analyses.

2. Materials and methods

2.1. Animal and experimental design

Four-week-old male ICR mice were purchased from Japan SLC (Japan) and maintained on a powdered basal diet (MF; Oriental Yeast, Japan) and tap water until they were 5-weeks-old; the study was started at this stage. The mice were housed in polycarbonate cages with paper beddings under standard conditions (room temperature, 22 ± 2 °C; relative humidity, 55 ± 5%; light/dark cycle, 12 h).

For the first investigation involving gene expression in the DC-treated liver, the mice were fed on the powdered diet containing DC (Novartis Animal Health, Switzerland) at 0 or 1500 ppm for 2 weeks (Exp. I). On the base of Exp. I, a two-stage liver carcinogenesis model in mice was employed in this study for

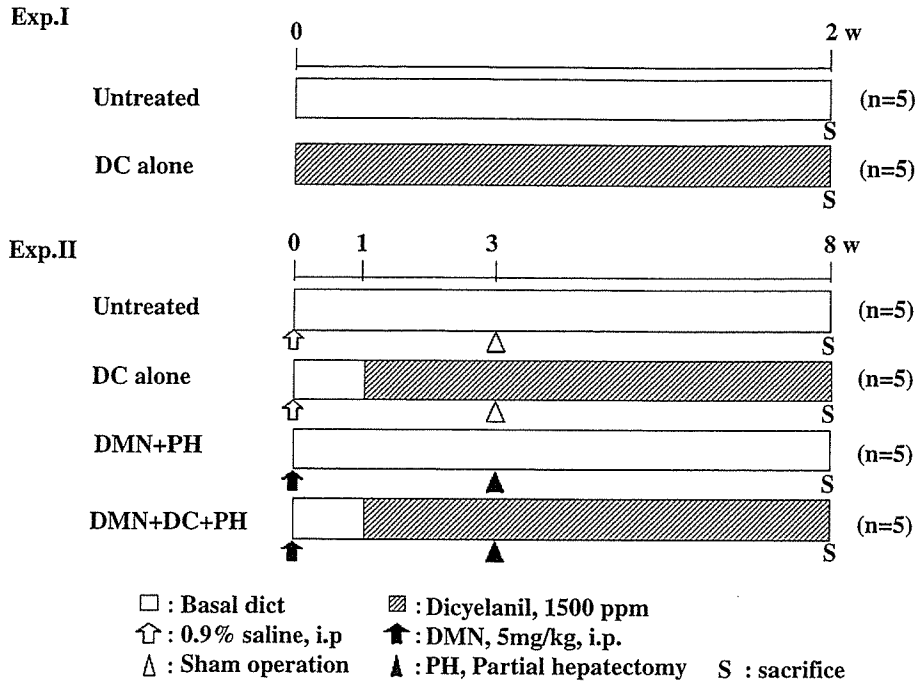

Fig. 1. Experimental designs of Exp. I and II.

the subsequent gene investigations (Fig. 1). To initiate hepatocarcinogenesis, a single i.p. injection of *N*-dimethylnitrosamine (DMN: Nakalai Tesque, Japan) at a dose of 0 (vehicle: 0.9% saline) or 5 mg/kg body weight was administered to the animals. After the 1-week recovery period, the mice were fed the powdered diet containing DC at the concentration of 0 or 1500 ppm. To enhance hepatocellular proliferation in the liver, these mice were subjected to two-thirds partial hepatectomy (Tsuda et al., 1979) at week 3 and maintained up to week 8 to determine pre-neoplastic foci (Exp. II).

At necropsy, the mice were sacrificed at each time point (2 weeks in Exp. I and 8 weeks in Exp. II) under anesthesia with ether by exsanguination from the abdominal aorta for sampling of the liver. Tissue samples for all analyses in Exp. I and II were collected from the right lateral robe of the liver in mice. One section of each liver was fixed with natural-buffered formalin for the histochemical analysis, and another section was embedded in the OCT compound (Tissue-Tek: Miles, USA) to freeze it for evaluation of γ-glutamyltransferase (GGT) positive foci—a marker of pre-neoplastic foci—in the mice liver (Cater et al., 1985). The remaining liver samples were weighed, frozen in liquid nitrogen, and stored at −80 °C until subsequent RNA isolation and protein extraction was performed.

These experiments were carried out in accordance with the Guide for Animal Experimentation by the Tokyo University of Agriculture and Technology.

2.2. *RNA isolation and cDNA microarray analysis*

In Exp. I, a large-scale analysis of gene expression was performed using Atlas Glass Microarray Mouse 3.80 I Microarray (BD Biosciences Clontech Nippon Becton Dickinson, Japan) for spotting 3757 genes. In summary, the total RNA was isolated using TRIzol reagent, according to the manufacturer's protocol (Invitrogen, USA). The total RNA sample was pooled from 3 animals of each group, and the production of labeled cDNA probe, hybridization, and imaging data analysis for the comparison between 0 and 1500 ppm groups were performed by BD Biosciences Clontech Nippon Becton Dickinson Co. Ltd., using Atlas Image and Data Analysis Software.

Exp. II uses the two-stage hepatocarcinogenesis model. Based on the results of the gene expression analysis obtained from Exp. I, two types of pathway-specific microarrays (Mouse Stress and Toxicity PathwayFinder Gene Array and Mouse Drug

Metabolism Gene Array: GEArray; SuperArray Bioscience, USA) were performed using biotinylated cDNA with 5 μg of RNA; hybridization and chemiluminescence detection were performed using a Bio Imaging System (Lab Works 4.0: UVP, USA) according to the manufacturer's protocol. The image data obtained from GEArray were analyzed using ScanAlyze (http://rana.lbl.gov/EisenSoftware.htm). To minimize the effects of measurement variation introduced by artificial sources in analyzed data of the microarrays in Exp. I and II, genes which were up- or down-regulated at least more than 2-fold were included.

2.3. RT-PCR and real-time RT-PCR

In Exp. I, the results of the cDNA microarray were validated using the conventional reverse transcriptional polymerase chain reaction (RT-PCR) of RNA samples obtained from all the animals used in this experiment. Reverse transcription was carried out with 1 μg of RNA for cDNA synthesis using ThermoScript RT-PCR System (Invitrogen, USA) according to the manufacturer's protocol, and the cDNA aliquots were used in subsequent PCR runs with each primer set under the optimal conditions (Table 2). Band intensities obtained by electrophoresis on 2% agarose gel were analyzed using the NIH Image. Band intensities of target genes were corrected based on those of β-actin in the same cDNA sample.

In the two-stage hepatocarcinogenesis model, quantitative real-time RT-PCR with SYBR Green was performed using ABI Prism 7000 Sequence Detection System (Applied Biosystems, USA) to validate the microarray (GEArray) results. The cDNA synthesis using RNA of all the animals was performed in the same manner as Exp. I. The PCR reaction was performed according to the SYBR Green PCR master mix protocol, and it was repeated twice in triplicate for each gene. The PCR primers were designed using Primer Express software (Applied Biosystems, USA).

2.4. Histological, histochemical, and immunohistochemical evaluations

Formalin-fixed liver tissues were embedded in paraffin, sectioned, and stained with hematoxylin and eosin (H-E) for the histological examinations. Additionally, immunohistochemical staining of proliferating cell nuclear antigen (PCNA) antibody (PC10; DakoCytomation, Japan) was performed by the avidin-biotin-peroxidase complex method. The histochemical staining of GGT was performed by modifying the methods proposed by Rutenberg et al. (1969). The frozen tissues were cryosectioned and fixed using methanol. After air-drying, the freshly prepared solution containing the substrate L-glutamic acid-γ-(4-metoxy-β-naphthylamide) (Sigma–Aldrich, USA) and fast blue BBN (Wako Pure Chemical Industries, Japan) in 0.1 M Tris-buffered saline (pH 7.4) was coated onto the section. Following the incubation, the slides were transferred into a 0.1 M cupric sulfate solution. These sections were then stained with hematoxylin, and mounted in 10% glycerol. The number of PCNA-positive cells per 200–300 cells in each slide was counted from five different areas to obtain the PCNA labeling index (PCNA LI). The number of GGT-positive cells per area was calculated from the number of positive cells in all lobes on the slide and from the total area in all lobes measured using the computer-assisted image analyzer (NIH image).

2.5. Assay of activated NF-κB

Proteins were extracted from the frozen liver tissue using PRO-PREP protein extract solution (iNtRON Biotechnology, Korea). After the protein concentration measurements using the BCA Protein Assay Kit (PIERCE Biotechnology, USA), the concentrations of total and active NF-κB were determined using an enzyme immunoassay kit (Oxford Biochemical Research, USA) according to the manufacturer's protocol.

2.6. Statistical evaluation

The data were presented as the mean + S.D. Statistical analysis was performed with the statistical software (JMP 4.0.5J, SAS Institute, USA). In Exp. I, the PCR data were compared between two groups using Student's *t*-test after one-way ANOVA. In Exp. II, the data of GGT, PCNA, PCR and NF-κB were compared between two corresponding groups using Student's *t*-test after the one-way ANOVA. Additionally, Dunnett's test was used to isolate the group(s) that differed significantly from the untreated group. A *P*-value of less than 0.05 was considered to be statistically significant.

Table 1
List of genes which were observed the fluctuation$_{(>2\text{-fold})}$ on a large-scale microarray of the DC group in Exp. 1

Accession number	Classification	Gene name	Ratio (DC/Untreated)	Function (activity)
Up-regulation				
	Xenobiotic metabolism			
NM_007815		Cytochrome P450, family 2, subfamily c, polypeptide 29	4.1	Oxidoreductase, Monooxygenase
NM_009993		Cytochrome P450, family 1, subfamily a, polypeptide 2	3.6	Oxidoreductase, Monooxygenase
NM_009467		UDP-glucuronosyltransferase 2 family, member 5	2.1	Glucuronosyltransferase
NM_007817		Cytochrome P450, family 2, subfamily f, polypeptide 2	2.0	Oxidoreductase, Monooxygenase
NM_007940		Epoxide hydrolase 2, cytoplasmic	2.0	Epoxide hydrolase
NM_007621		Carbonyl reductase 2	2.0	Oxidoreductase, Carbonyl reductase
	Simple carbohydrate metabolism			
NM_008062		Glucose-6-phosphate dehydrogenase X-linked	3.0	Oxidoreductase, Glucose-6-phosphate 1-dehydrogenase
NM_008061		Glucose-6-phosphatase, catalytic	2.4	Oxidoreductase, Glucose-6-phosphate 1-dehydrogenase
	Energy metabolism			
NM_008063		Glucose-6-phosphatase, transport protein 1	2.3	Oxidoreductase, Glucose-6-phosphate 1-dehydrogenase
NM_013467		Aldehyde dehydrogenase family 1, subfamily A1	5.9	Acyltransferase, Carnitine O-palmitoyltransferase
	Simple lipid metabolism			
NM_011044		Phosphoenolpyruvate carboxykinase 1, cytosolic	2.0	Carboxy-lyase, GTP binding
NM_009948		Carnitine palmitoyltransferase 1, muscle	3.3	Acyltransferase, Carnitine O-palmitoyltransferase
NM_008097		Glutaryl-Coenzyme A dehydrogenase	2.0	Oxidoreductase, Acyl-CoA dehydrogenase, Glutaryl-CoA dehydrogenase,
	Cholesterol metabolism			
NM_015729		Acyl-Coenzyme A oxidase	2.0	Oxidoreductase, acyl-CoA oxidase
	Amino acid metabolism			
NM_019709		Site-1 protease	2.7	Serine-type endopeptidase activity
NM_007482		Arginase 1, liver	2.4	Arginase, Manganese ion binding
	Metabolism of cofactors, vitamins, and related substrates			
NM_009804		Catalase 1	2.0	Oxidoreductase, Acting on peroxide as acceptor, Peroxidase
NM_008160		Glutathione peroxidase 1	3.0	Oxidoreductase, Glutathione peroxidase

Table 1 (*Continued*)

Accession number	Classification	Gene name	Ratio (DC/Untreated)	Function (activity)
NM_007757		Coproporphyrinogen oxidase	2.1	Oxidoreductase, Coproporphyrinogen oxidase
	Other metabolism enzymes			
NM_008162		Glutathione peroxidase 4	2.0	Oxidoreductase, Glutathione peroxidase
NM_009286		Sulfotransferase, hydroxysteroid preferring 2	3.4	Alcohol sulfotransferase
NM_019946		RIKEN cDNA 1500002K10 gene	3.3	Microsomal glutathione transferase
NM_008184		Glutathione *S*-transferase, mu 6	3.2	Glutathione transferase
NM_010001		Cytochrome P450, family 2, subfamily c, polypeptide 37	3.1	Oxidoreductase, Monooxygenase
NM_010010		Cytochrome P450, 46 (cholesterol 24-hydroxylase)	2.9	Oxidoreductase, Monooxygenase
NM_009127		Stearoyl-Coenzyme A desaturase 1	2.6	Oxidoreductase, Stearoyl-CoA 9-desaturase
NM_011933		2-4-dienoyl-Coenzyme A reductase 2, peroxisomal	2.2	Oxidoreductase, peroxisome organization
NM_010240		Ferritin light chain 1	2.2	Ferric iron binding
NM_015762		Thioredoxin reductase 1	2.2	Oxidoreductase, Acting on NADH or NADPH, disulfide as acceptor, Thioredoxin-disulfide reductase
NM_007750		Cytochrome c oxidase, subunit VIIIa	2.0	Oxidoreductase, cytochrome-c oxidase
	Basic transcription factor			
NM_008712		Nitric oxide synthase 1, neuronal	2.0	Oxidoreductase, calmodulin binding, Nitric-oxide synthesis
	CDK inhibitor			
NM_010866		Myogenic differentiation 1	4.1	DNA binding, Protein binding
	Other cell adhesion protein			
NM_007670		Cyclin-dependent kinase inhibitor 2B (p15, inhibits CDK4)	2.4	Cyclin-dependent protein kinase inhibitor, Transcription factor
	Major histo-compatibility complex			
NM_010796		Macrophage galactose *N*-acetyl-galactosamine specific lectin	2.2	Sugar binding
	Extracellular transport/carrier proteins			
NM_009735		Beta-2 microglobulin	2.1	MHC class I receptor
NM_013465		Alpha-2-HS-glycoprotein	2.6	Cysteine protease inhibitor
	Oncogenes and tumor suppressors			
NM_007469		Apolipoprotein CI	2.3	Lipid transporter activity

Table 1 (*Continued*)

Accession number	Classification	Gene name	Ratio (DC/Untreated)	Function (activity)
	Trafficking/ targeting protein			
NM_008502		Lethal giant larvae homolog	2.6	Maintenance of apical/basal cell polarity
NM_008997		RAB11B, member RAS oncogene family	2.4	DNA binding, GTP binding
	Ribosomal protein			
NM_009228		Syntrophin, acidic 1	2.3	Actin binding, calmodulin binding, Protein binding
	RAN processing, turnover, and transport			
NM_009081		Ribosomal protein L28	3.5	Structural constituent of ribosome
	Chromatin protein			
NM_008774		Poly A binding protein, cytoplasmic 1	3.2	RNA binding
	Growth factors, cytokines, and chemokines			
NM_007690		Chromodomain helicase DNA binding protein 1	3.1	ATP-dependent helicase activity, Chromatin binding, Nucleic acid binding
NM_009142		Small inducible cytokine subfamily D, 1	2.7	Chemokine, Cytokine
	Intracellular transducers/ effectors/ modulators			
NM_009131		Stem cell growth factor	2.1	Growth factor, Nucleic acid binding
NM_009059		Ral guanine nucleotide dissociation stimulator,-like 2	2.5	Guanyl-nucleotide exchange factor
NM_009412		Tumor protein D52	2.1	Unknwon
	Proteosomal protein			
NM_007791		Cysteine rich protein	2.0	Protein binding, Zinc ion binding
NM_011189		Protease (prosome, macropain) 28 subunit, alpha	3.7	Unknwon
	Unclassified			
NM_011192		Proteaseome (prosome, macropain) 28 subunit, 3	3.3	Proteasome activator
NM_019749		Gamma-aminobutyric acid receptor associated protein	3.6	Microtubule binding, microtubule cytoskeleton organization and biogenesis
NM_016774		ATP synthase, H+ transporting mitochondrial F1	3.1	ATP biosynthesis, Hydrogen-exporting ATPase activity, phosphorylative and rotational mechanism
NM_019689		Dead ringer homolog 2 (*Drosophila*)	3.1	DNA binding, intracellular
NM_020287		Insulinoma-associated 2	3.1	Unknwon
NM_015755		Hormonally up-regulated Neu-associated kinase	3.0	Protein kinase, Protein amino acid phosphorylation
NM_008226		Hyperpolarization-activated, cyclic nucleotide-gated K + 2	2.9	3′,5′-cAMP binding, potassium channel

Table 1 (*Continued*)

Accession number	Classification	Gene name	Ratio (DC/Untreated)	Function (activity)
NM_007448		Angiogenin related protein 2	2.7	Endonuclease, negative regulation of protein biosynthesis
NM_008075		Gamma-aminobutyric acid (GABA-A) receptor, subunit rho 1	2.6	GABA-A receptor, Ion channel, Neurotransmitter receptor activity
NM_010827		Musculin	2.6	Regulation of transcription, DNA-dependent
NM_013610		Ninjurin 1	2.6	Protein binding, tissue regeneration
NM_011097		Paired-like homeodomain transcription factor 1	2.6	Regulation of transcription, DNA-dependent
NM_011662		TYRO protein tyrosine kinase binding protein	2.6	Protein binding
NM_011912		Ventral anterior homeobox containing gene 2	2.6	Transcription factor activity
NM_008074		GABA-A receptor, subunit gamma 3	2.5	GABA-A receptor, Ion channel, Neurotransmitter receptor activity
NM_015740		General control of amino acid synthesis-like 1 (yeast)	2.5	Protein binding
NM_019917		Tissue-type vomeronasal neurons putative pheromone receptor	2.5	Receptor activity
NM_010896		Neurogenic differentiation 3	2.4	DNA binding, cell differentiation
NM_020012		Ring finger protein 14	2.4	Ubiquitin-protein ligase activity
NM_009429		Translationally regulated transcript (21 kDa)	2.4	Calcium ion binding, anti-apoptosis
NM_011918		Z-band alternatively spliced PDZ-motif protein	2.4	Protein binding
NM_008423		Potassium voltage gated channel, Shal-related family, member 1	2.3	Voltage-gated potassium channel
NM_008857		Protein kinase C, lamda	2.3	ATP binding, Diacylglycerol binding, Protein serine/threonine kinase, Transferase
NM_011862		Protein kinase C and casein kinase substrate in neurons 2	2.3	Cytoskeletal protein binding
NM_019517		Beta-site APP-cleaving enzyme 2	2.2	Aspartic-type endopeptidase,
NM_009902		Claudin 3	2.2	Structural molecule
NM_009903		Claudin 4	2.2	Structural molecule
NM_019626		Cerebellin 1 precursor protein	2.2	Extracellular space component
NM_008076		GABA-A receptor, subunit rho 2	2.2	GABA-A receptor, Ion channel, Neurotransmitter receptor activity
NM_008479		Lymphocyte-activation gene 3	2.2	Defense response
NM_009156		SelenoproteinW, muscle 1	2.2	Selenium binding
NM_010162		Exostoses (multiple) 1	2.1	Transferase (transferring glycosyl groups)
NM_010425		Forkhead box D3	2.1	DNA binding, transcription factor
NM_016705		Kinesin family member 21A	2.1	Microtubule motor activity
NM_011195		Pre T-cell antigen receptor alpha	2.1	Extracellular space
NM_019516		Galectin-related inhibitor of proliferation 1	2.0	lactose binding, induction of apoptosis by intracellular signals
NM_010286		Glucocorticoid-induced leucine zipper	2.0	Regulation of transcription, anti-apoptosis
NM_008935		Prominin	2.0	Phototransduction
NM_019974		Protease, serine, 20	2.0	Serine-type endopeptidase, proteolysis and peptidolysis